Molecular cloning and functional analyses of an adhesion molecule, neuroglian, in *Mythimna separata* (Lepidoptera: Noctuidae)

Kakeru YOKOI*, Yoshiaki KATO**, Masahiro SUZUKI and Ken MIURA

Applied Entomology, Graduate School of Bio-Agricultural Sciences, Nagoya University, Chikusa, Nagoya 464-8601, Japan;
e-mails: yokoi123@affrc.go.jp, m____sssuzuki@gmail.com, k-miura@agr.nagoya-u.ac.jp

Abstract. Insect cellular immune reaction, which generally includes phagocytosis, encapsulation and nodule formation, is achieved by hemocytes circulating in insect haemolymph. The shift of hemocytes from the normal phase to the adhering phase is an important process in the cellular immune reaction, which includes the attachment of hemocytes to foreign surfaces or other hemocytes via adhesion factors. Neuroglian is one of the adhering factors associated with encapsulation in *Manduca sexta* and *Drosophila melanogaster*. Here we studied the localization of neuroglian (MsNrg) in *Mythimna separata* and its functional role in the cellular immune reaction. The distribution of *MsNrg* mRNA between hemocyte populations was determined using real-time quantitative reverse transcription PCR and in situ hybridization, which revealed that *MsNrg* was highly expressed in adhering hemocytes, especially in plasmatocytes. Unexpectedly, the transcript was observed as well in non-adhering hemocytes, implying neuroglian has a function in non-adhering hemocytes. Moreover, we showed that the amount of *MsNrg* mRNA was not changed by injections of either biotic or abiotic non-selves. Fewer latex beads were fully encapsulated by hemocytes in larvae treated with *MsNrg* double-stranded RNA than in control larvae, but their ability to achieve phagocytosis and nodule formation remained unchanged by the *MsNrg* knockdown. These results indicate that the function of neuroglian in the cellular immune reaction is conserved in *D. melanogaster* and lepidopteran species, and neuroglian in non-adhering hemocytes could possess unidentified function.

INTRODUCTION

Insects do not have adaptive immune systems, which are based on genomic rearrangement of immune genes. Instead, they have quite robust innate immune systems, on which they solely rely. The latter immune system, like the former, consists of humoral and cellular defenses. The humoral immune defense of insects is composed of several distinct levels of reactions. For example, the invasion of pathogens induces the production of several antimicrobial peptides and reactive oxygen/nitrogen species (Lemaitre & Hoffmann, 2007). Molecular mechanisms and pathways of insect humoral immune defense have been studied intensively in a model insect, *Drosophila melanogaster* Meigen (Diptera: Drosophidae). Cellular immune defense is mediated mainly by hemocytes as shown in vertebrate systems (Lavine & Strand, 2002). These hemocytes can be divided into several distinct types according to their shapes and functions. In larval stages of typical lepido-

pteran insects, five types of hemocytes are usually found: plasmatocytes, granular cells, spherule cells, oenocytoids and prohemocytes. Plasmatocytes and granular cells are adhering hemocytes, which are considered to play a central role in cellular immune defense in Lepidoptera (Lavine & Strand, 2002). Insect cellular immune defense mainly consists of phagocytosis, encapsulation and nodulation. During phagocytosis, hemocytes engulf small abiotic (such as small chromatography beads) or biotic targets (microbes and apoptotic bodies) (Hernandez et al., 1999; Da Silva et al., 2000). In Lepidoptera, phagocytosis is carried out mainly by granular cells and plasmatocytes. Encapsulation is another cellular immune defense during which adhering hemocytes attach to non-self targets, which are too large to engulf (parasitoids, nematodes and large beads), and form multiple cell layers around them to physically isolate and kill the target (Lavine & Strand, 2002). Nodulation is initiated by small but numerous targets. In this case, hemo-

* Present address: Insect Genome Research and Engineering Unit, Division of Applied Genetics Institute of Agrobiological Sciences, National Agriculture and Food Research Organization (NARO), 1-2 Owashi, Tsukuba, Ibaraki, 305-8634, Japan; e-mail: yokoi123@affrc.go.jp

** Present address: BASF Japan Ltd., Roppongi Hills Tower 21F, 6-10-1 Roppongi, Minato-ku, Tokyo 106-6121, Japan; e-mail: Katoooooo@yahoo.co.jp

cytes attach to aggregated bacteria, which are eventually surrounded and killed by multiple cell layers, as is seen in the process of encapsulation (Lavine & Strand, 2002; Marmaras & Lampropoulou, 2009).

These cellular reactions are thought to be controlled by several cell adhesion molecules on the surfaces of hemocytes; these molecules are responsible for the shift between the non-adhesion and adhesion status of hemocyte (Nardi et al., 2005). Therefore, it is quite important to investigate cell adhesion molecules for understanding these cellular immune defense mechanisms. Although there is a large amount of information on the molecular mechanisms of humoral immune defense, the mechanisms of cellular immune defense, such as molecular basis for hemocyte aggregation and intercellular signalling, recognition of biotic or abiotic non-selves and regulation of hemocyte movements, are far from being described in detail.

We have been interested in the host regulation mechanisms exerted by parasitoid wasps against their host larvae in which parasitoid-derived factors are known to regulate the lepidopteran host's immune defenses (Suzuki et al., 2008). The target molecules of these parasitoid-derived factors could include adhesion molecules on the surfaces of the host's hemocytes. One of these adhesion molecules in the immunoglobulin superfamily is neuroglian (Hortsch, 1996; Wiegand et al., 2000; Nardi et al., 2003, 2005). Neuroglian was first reported in *D. melanogaster* (Bieber et al., 1989), and subsequently described in a lepidopteran, the tobacco hornworm, *Manduca sexta* (Linnaeus) (Lepidoptera: Sphingidae) (Chen et al., 1997). Neuroglian is homologous to vertebrate neural adhesion molecule Ll, and its expression was first shown in developing nerves of *D. melanogaster* (Bieber et al., 1989). Since then, main research interest in *Drosophila* neuroglian has been in the formation and growth of a synapse by using mutant fly lines and cultured cells (Hortsch et al., 1995; Hall & Bieber, 1997; Siegenthaler et al., 2015). In the meanwhile, Nardi, Kanost and co-workers noticed the occurrence of neuroglian proteins on the surfaces of the hemocytes of the lepidopteran, *M. sexta*, and reported its distribution in hematopoetic organs and its functional involvement in encapsulation (Nardi, 1994; Nardi et al., 2003, 2006; Zhuang et al., 2007). After the series of publications, involvement of *D. melanogaster* neuroglian in encapsulating a parasitoids wasp's egg was shown (Williams, 2009).

To extend the study of neuroglian's involvement in cellular immune defense, we first determined full nucleotide sequences of the *Mythimna separata* (Walker) (Noctuidae: Lepidoptera) *neuroglian* (*MsNrg*). Subsequently, we investigated the abundance and distribution of *MsNrg* mRNA in different types of hemocytes using real-time quantitative reverse transcription PCR (qRT-PCR). As functional assay of the involvement of MsNrg in cell-mediated immune responses in phagocytosis, encapsulation and nodulation, we conducted knockdown assays using RNA interference (RNAi).

MATERIALS AND METHODS

Insect rearing

M. separata was reared as described in Suzuki & Tanaka (2007) and Nakamatsu et al. (2006). Briefly *M. separata* were collected in cornfields in Kanoya, Kagoshima Prefecture, Japan. These insects were reared on an artificial diet (Insecta LFs, Nihon Nosan Co., Kanagawa Prefecture, Japan) under a long day photoregime (16L : 8D) at 25 ± 1°C.

RNA extraction and cDNA synthesis

The sixth instar, day-0 (VI-0, hereafter abbreviated in this manner) larvae were anesthetized with carbon dioxide gas. Their hemolymph was collected in ice-cold phosphate-buffered saline (PBS), and the total hemocytes were isolated by centrifugation at 2,200 rpm for 10 min at 4°C. Total RNA was extracted from these samples using TRIZOL reagent (Invitrogen, Carlsbad, CA, USA) according to the manufacturer's instructions. The first strand cDNA synthesis was done by either PrimeScript reverse transcriptase (TAKARA, Kusatsu, Shiga, Japan) or Thermoscript reverse transcriptase (Thermo Fisher Science, Waltham, MA, USA), primed with three distinct primers, random hexamer, oligo-(dT) 20 and a tagged oligo-(dT) primer. The sequence of the tagged oligo-(dT) primer used for 3' RACE is: 5'-CTACAGTCT-GCTCACAGCATAGTATTTTTTTTTTTTTTTTTTTTTTTTTTT-VN-3'. For 5' RACE, an RNA oligo (5'-AAGCAGUGGU-AUCAACGCAGAGUGGG-3') was included in the reverse transcription reaction according to the instruction of a SMART RACE cDNA amplification kit (Clontech, Mountain View, CA, USA).

Homologous RT-PCR methods

A pair of degenerate primers was designed based on the highly conserved regions of neuroglian proteins from four species of insects, *D. melanogaster*, *Bombyx mori* Linnaeus (Lepidoptera: Bombycidae), *M. sexta* and *Apis mellifera* Linnaeus (Hymenoptera: Apidae), 5'-ATGACKYTNGAYCCIGARGGIAA-3' for a forward primer and 5'-CAKCCRTARTTICCIGTRTCYTT-3' for a reverse primer. PCR following RT-PCR was performed using the oligo-(dT) 20 -primed first strand cDNA as described above under the following conditions: the reaction mixture was first kept at 94°C for 2 min, followed by 35 cycles of denaturation at 94°C for 30 s, annealing at 45°C for 1 min and extension at 72°C for 1 min. A random hexamer-primed first strand cDNA preparation was also utilized to amplify a different region, closer to the 3' end of the putative neuroglian cDNA. In this case, reverse transcription was carried out using a thermostable enzyme, Thermoscript reverse transcsriptase at 65°C, following 10 min incubation at 25°C. RT-PCR was then performed with another pair of degenerate primers: 5'-GTNYTNACIGGITAYAARATITAYTA-3' as the forward primer and 5'-TCKCKRTCRTGIACRTCRTAITT-3' as the reverse primer. The thermal cycling conditions were as follows: 94°C for 2 min, followed by 43 cycles of denaturation at 94°C for 30 s, annealing at 50°C for 1 min and extension at 72°C for 1 min. Respective PCR products were fractionated using agarose gel electrophoresis, and the cDNAs with expected sizes were recovered using a QIAquick Gel Extraction kit (QIAGEN, Hilden, North Rhine-Westphalia, Germany). The cDNA fragments were sub cloned into either pBluescript II SK+ (Stratagene, La Jolla, CA, USA) or pCR2.1-TOPO (Invitrogen). Several independent cDNA clones were sequenced using an ABI Prism Dye Terminator Cycle Sequencing kit and a DNA Sequencer (Model 3130, Applied Biosystems, Waltham, MA, USA).

Acquisition of *neuroglian* full nucleotide sequence by PCR-based methods

The two partial sequences obtained from different regions of *MsNrg* using homologous RT-PCR procedures were used to design gene-specific primers (forward primer: 5'-GGC-GAGTCAGCTGAGATCAAG-3', reverse primer: 5'-CTCCT-TAGCTGGTAAAGTACTC-3') to clone the unidentified region between the two sequences. The RT-PCR products were separated on an agarose gel, and the cDNA with the expected size was recovered. The cDNA fragment was sequenced directly by primer walking.

Amplifying the *MsNrg* cDNA in the vicinity of its putative 3' end after a conventional reverse transcription reaction presented a technical challenge. Therefore, for 3' RACE, Thermoscript reverse transcsriptase was used for reverse transcription at a higher temperature. The reverse transcription reaction was primed with the tagged anchor primer at 42°C for 7 min, and this was followed by incubation at 65°C for 60 min. This cDNA template was used for the following 3' RACE with a gene-specific primer (5'-TACCATTGACGGCCCCATAGTGAA-3') and a 3' anchor primer (5'-CTACAGTCTGCTCACAGCATAGTA-3') under the following conditions: 94°C for 2 min, followed by 35 cycles of denaturation at 94°C for 30 s, annealing at 68°C for 30 s and extension at 72°C for 1 min 20 s. The PCR products were fractionated on an agarose gel, and the cDNA fragments corresponding to the expected sizes (600–800 bp) were recovered. The secondary PCR was done using these cDNA fractions with the 3' anchor primer and a nested gene specific primer (5'-CATAGTGAAGC-CGGACGAGGACA-3'). The thermal cycles used were: 94°C for 2 min, followed by 45 cycles of denaturation at 94°C for 30 s, annealing at 68°C for 30 s and extension at 72°C for 1 min. The secondary PCR products were separated by agarose gel electrophoresis, and analyzed by Southern blotting. The 660 bp cDNA fragment (see Fig. 1) was used as a probe. A Gene Image Detection Kit (GE Healthcare UK Ltd, Amersham Place, England) was used for probe labelling and detection. The cDNA zone exhibiting a positive signal was recovered and sub cloned. Then, the positive colonies were identified by hybridization using the probe mentioned above, the plasmids were prepared, and their cDNA inserts were sequenced.

5' RACE was done by using a 5' anchor primer (5'-AA-GCAGTGGTATCAACGCAGAGT-3') and a gene specific primer (5'-GTAGTCGAACGGTTTGCCGTTC-3') designed from the 670 bp region (see Fig. 1) under the following conditions: 94°C for 2 min, followed by 35 cycles of denaturation at 94°C for 30 s, annealing at 65°C for 30 s, and extension at 72°C for 1 min. For preparation of the template, see "RNA extraction and cDNA synthesis" section in "Material and methods".

The PCR products were fractionated on an agarose gel, and the cDNA band with the expected size was recovered and sequenced directly.

Sequence analyses

The editing and analyses of nucleotide and amino acid sequences were performed using GENETYX software (GENE-TYX corporation, Tokyo, Japan). Homology search and multiple alignment were performed using CLUSTAL W and BLAST programmes on the DNA Data Bank of Japan website (http://clustalw. ddbj.nig.ac.jp/top-j.html). Accession numbers of *M. sexta Nrg* and *D. melanogaster Nrg* are U50719.1 and NM_001169234, respectively. Domain analysis was done using NCBI Conserved Domain Search programme on the National Center for Biotechnology Information website (Marchler-Bauer et al., 2017).
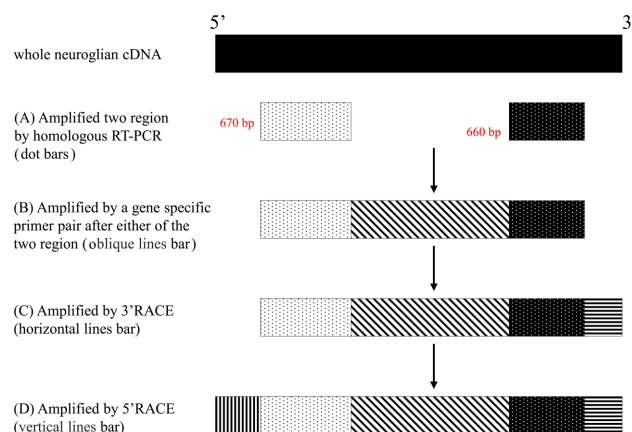

Fig. 1. Schematic drawing showing steps used in obtaining the full-length sequence. The top grey bar indicates the complete *neuroglian* cDNA. (A) Open and filled bars indicate the two regions obtained using homologous RT-PCR. Expected sizes for respective cDNA fragments are also shown. (B) The region between the two cDNA fragments (A) was amplified using conventional PCR methods and sequenced directly (diagonally hatched bar). (C) A gene specific primer was designed based on the 670 bp region (open bar) and used for the 5' RACE (vertically hatched bar). (D) Design of gene specific primers for 3' RACE and nested PCR was based on the sequence in the cDNA fragment indicated by the filled zone. This 660 bp cDNA fragment was also used as a probe for Southern blotting. The region determined by the 3' RACE is indicated as a horizontally hatched bar. For the amplification of the 660 bp fragment and the extreme 3' region, a thermostable reverse transcriptase was utilized. For details, see "Homologous RT-PCR methods" section of "Material and Methods".

RNA interference

Double-stranded RNA (dsRNA) was prepared as follows. First, T7 RNA polymerase promoter sequences were introduced into both 5' ends of the neuroglian double strand cDNA fragment (Fig. 2, DNA sequences are underlined) using PCR with the following primer pair: 5'-taatacgactcactatagggACGGGTATCGCGTC-TACATT-3'; 5'-taatacgactcactatagggTTGGTGATGACGATG-GTGTT-3'. The T7 RNA polymerase promoter sequences are in lower case. The T7 promoter-tagged cDNA was purified using a QIAquick PCR Purification kit (QIAGEN) and used as a template for dsRNA synthesis using a MEGAscript RNAi kit (Ambion, Carlsbad, CA, USA). For negative control, a dsRNA fragment possessing a partial *enhanced green fluorescent protein* (*EGFP*) sequence was also prepared in the same fashion by using the pEGFP-N1 plasmid (Clontech).

qRT-PCR

mRNA amounts were estimated using qRT-PCR. Hemolymph from four to six larvae was collected in Sf900 III media (Invitrogen) and was seeded in a 50-ml culture bottle. The hemocytes were allowed to attach the bottle for 30 min, and non-adhering hemocytes were detached by tapping the bottle while leaving adhering ones attached. Total RNA was extracted separately from either the adhering or non-adhering hemocyte preparations. Total RNA was also extracted from the granular cell monolayer and plasmatocyte-enriched monolayer. Isolation of granular cells and plasmatocytes was done according to Suzuki et al. (2009). Reverse transcription of 1 µg each of total RNA was primed by random hexamers. Each real-time RT-PCR reaction mixture (12.5 µl) included 0.5 µl of 1st strand cDNA, and the real-time detection and analyses were done based on SYBR green dye chemistry using a SYBR Premix Ex *Taq* Perfect Real Time kit (TAKARA). The thermal cycling conditions used for *MsNrg* analysis were:

Fig. 2. Full nucleotide (upper) and predicted amino acid (lower) sequences of *MsNrg* cDNA. Nucleotides are numbered from the first base at the 5' end. Amino acids are numbered from the initiating methionine residue. The polyadenylation signal atgaaa is designated by lower case letters. Amino acid residues, which may form a transmembrane domain, are in bold italics. The cDNA sequence used to synthesize *MsNrg* double strand RNA is underlined. The position of primer pair used for qRT-PCR is indicated by bold case letters.

95°C for 10 s, then 40 cycles of 95°C for 5 s, 60°C for 30 s; this was followed by dissociation analysis composed of 95°C for 15 s, 60°C for 30 s, then a shallow thermal ramp to 95°C. The following primer pair was used: forward primer, 5'-CTCGTAAC-GACGCGAGTGTAA-3'; reverse primer, 5'-CGTCTCCGT-CACTTGCAGATA-3'. The other primer pair for amplifying the house keeping gene [ribosomal protein L32 (*RPL32*)] was used under the same conditions. Each primer sequence was: 5'-GGT-TACGGTTCAAACAAGAAGAC-3' for forward primer; 5'-TC-CTGTTCTGCATCATCAGGAT-3' for reverse primer. Relative quantification for each mRNA was done based on a threshold cycle number determined by the second derivative of each primary amplification curve. The obtained mRNA values were normalized according to amount of RPL32 expressions or number of cells in the respective preparations.

In situ hybridization

In situ hybridization was done as described in Kato et al. (2014). The sequences of *MsNrg* antisense and *MsNrg* sense probes are 5'-CGTGGGGGGTACCGGAGGCTTCGCACTT-GATCTCAGCTGACTCGCCTTCCGCGAGG-3' and 5'-CCTCGCGGAAGGCGAGTCAGCTGAGATCAAGTGCGAA-GCCTCCGGTACCCCACG-3, respectively.

Phagocytosis assay

The V-1 larvae were injected with 1 µg of either *MsNrg* or *EGFP* dsRNA. Two days later, these larvae (ecdysed to VI-0 larvae) were injected with 5×10^6 DH5 alpha *Escherichia coli* labelled with fluorescein isothiocyanate (FITC). Three hours later, the hemocytes were collected and resuspended in HEPES-buffered saline (HBS, 37.5 mM Hepes buffer, pH 7.4, 100 mM NaCl, 2 mM CaCl₂) containing 8% (v/v) saturated phenylthiourea. These hemocyte suspensions were put on glass slides and left for 15 min. Then, they were washed three times with HBS, fixed in 70% EtOH for 20 min, washed three times with HBS again, and then mounted in HBS containing 40% glycerol. Five fields of view were randomly chosen per glass slide and the percentage of FITC-positive hemocytes, which had engulfed the labelled *E. coli*, was calculated after observation through a fluorescent microscope equipped with Nomarski optics (Olympus, Model BX41, Tokyo, Japan).

Nodulation assay

V-1 larvae were injected with the dsRNAs. Two days later, the larvae were further injected with formaldehyde-fixed DH5 alpha *E. coli* at a dosage of 3×10^7 pfu. Twenty-four hours after injection with *E. coli* each larva was dissected, and the number and morphology of the nodules formed were recorded.

Encapsulation assay

Two days after being treated with dsRNA, VI-0 larvae were injected with ca. 20 fluorescent latex beads (Fluoresbrite Plain Microspheres, 20 µm in diameter, YG in color, Polysciences, Inc., Warrington, PA, USA). Twelve hours after the injection of beads, the larvae were dissected under a fluorescent stereoscopic microscope (Olympus, Model SZX12) and the fluorescent beads were recovered. The recovered beads were then observed using a microscope equipped with Nomarski optics, classified into three categories based on the degree of encapsulation and frequency of each of the following categories was determined: category A, beads surrounded by more than ten layers of flattened cells; category B, beads surrounded by only a few cell layers; category C, naked beads or those with only a few attached cells.

RESULTS

cDNA cloning and sequence analyses of *MsNrg*

To obtain a full nucleotide sequence of *MsNrg* cDNA, we started with a homologous RT-PCR approach based on the amino acid sequences of insect neuroglian proteins so far reported. Two pairs of degenerate PCR primers, one of which was used for the amplification of the region located in the N-terminal and the other for the region in the C-terminal half, were synthesized and used for RT-PCR with oligo-(dT) primed 1st strand cDNA prepared from total hemocyte RNA. The former region (open bar in Fig. 1, about 670 bp) was successfully amplified while the latter region (filled bar in Fig. 1, about 660 bp) was not. We considered the possibility that strong secondary structures of *MsNrg* mRNA might have interfered with the reverse transcription of this region. To circumvent this potential
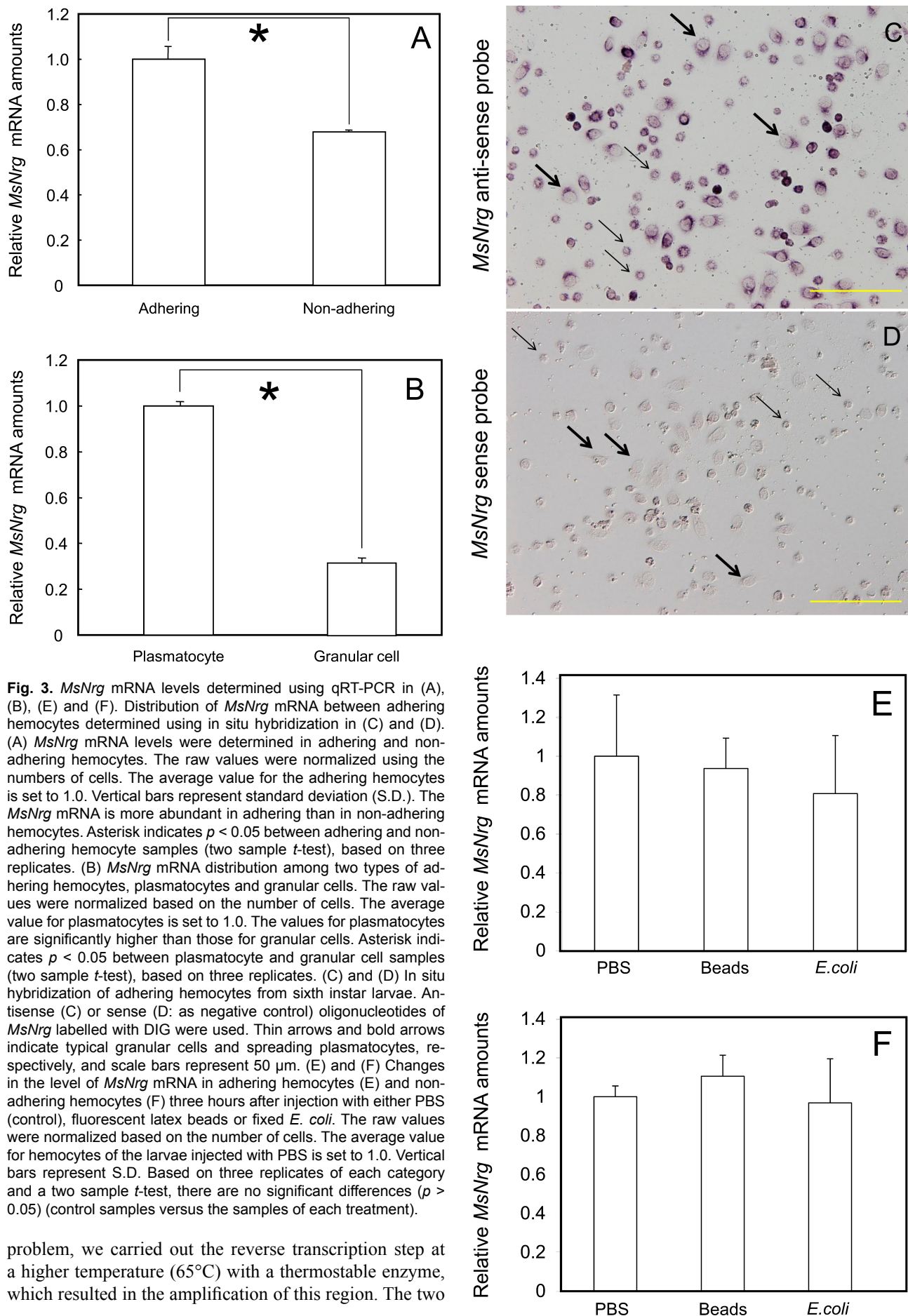
Fig. 3. *MsNrg* mRNA levels determined using qRT-PCR in (A), (B), (E) and (F). Distribution of *MsNrg* mRNA between adhering hemocytes determined using in situ hybridization in (C) and (D). (A) *MsNrg* mRNA levels were determined in adhering and non-adhering hemocytes. The raw values were normalized using the numbers of cells. The average value for the adhering hemocytes is set to 1.0. Vertical bars represent standard deviation (S.D.). The *MsNrg* mRNA is more abundant in adhering than in non-adhering hemocytes. Asterisk indicates $p < 0.05$ between adhering and non-adhering hemocyte samples (two sample *t*-test), based on three replicates. (B) *MsNrg* mRNA distribution among two types of adhering hemocytes, plasmatocytes and granular cells. The raw values were normalized based on the number of cells. The average value for plasmatocytes is set to 1.0. The values for plasmatocytes are significantly higher than those for granular cells. Asterisk indicates $p < 0.05$ between plasmatocyte and granular cell samples (two sample *t*-test), based on three replicates. (C) and (D) In situ hybridization of adhering hemocytes from sixth instar larvae. Antisense (C) or sense (D: as negative control) oligonucleotides of *MsNrg* labelled with DIG were used. Thin arrows and bold arrows indicate typical granular cells and spreading plasmatocytes, respectively, and scale bars represent 50 μm. (E) and (F) Changes in the level of *MsNrg* mRNA in adhering hemocytes (E) and non-adhering hemocytes (F) three hours after injection with either PBS (control), fluorescent latex beads or fixed *E. coli*. The raw values were normalized based on the number of cells. The average value for hemocytes of the larvae injected with PBS is set to 1.0. Vertical bars represent S.D. Based on three replicates of each category and a two sample *t*-test, there are no significant differences ($p > 0.05$) (control samples versus the samples of each treatment).

problem, we carried out the reverse transcription step at a higher temperature (65°C) with a thermostable enzyme, which resulted in the amplification of this region. The two

cDNA fragments were sub cloned and sequenced, revealing that these fragments encoded portions of the MsNrg polypeptide. Then, the unidentified region between the two sequences (diagonally hatched bar in Fig. 1) was amplified with a gene specific primer pair whose design was based on the sequences of the 660 and 670 bp regions. The amplified fragment was gel-purified and sequenced directly.

The first strand cDNA used for 5' RACE was synthesized with oligo-(dT) priming under the presence of an RNA oligo bearing the 5' anchor sequence described in the Materials and Methods. This cDNA preparation was subjected to RT-PCR with the 5' anchor primer and a gene specific primer, yielding a single cDNA band with an apparent size of 1 kbp. The cDNA fragment was sequenced directly, giving the extreme 5' end sequence of *MsNrg* cDNA (vertically hatched bar in Fig. 1).

To amplify the extreme 3' region (horizontally hatched bar in Fig. 1), reverse transcription was done at 65°C using the thermostable enzyme with the tagged oligo-(dT) primer. The following RT-PCR resulted in relatively poor amplification and banding. So, we utilized Southern hybridization to identify the positive cDNA band on a gel and selected the positive colonies after the sub cloning procedure. Then, a few independent clones were sequenced, and the consensus sequence for the extreme 3' end was determined. These respective sequences were combined, giving the full nucleotide sequence for *MsNrg* cDNA. The whole sequence data was registered in Genbank (accession no. AB490501).

Complete cDNA and predicted amino acid sequences of MsNrg are shown in Fig. 2. The cDNA consists of 4,130 bp without its poly(A) tail. It has a 5' untranslated region (UTR) of 148 bp and a 3' UTR of 220 bp. The 3' UTR contained a polyadenylation signal (agtaaa) 26 bp upstream from the polyadenylation site (Beaudoing et al., 2000). The cDNA encodes an 1,254 amino acid-polypeptide with a predicted molecular mass of 140, 020.58 Da.

The predicted amino acid sequence of MsNrg was aligned with the counterparts of *M. sexta* Nrg and *D. melanogaster* Nrg using the CLUSTAL W program at the DNA data bank of Japan website (data not shown). Amino acid residues were highly conserved in the *M. sexta* Nrg and *D. melanogaster* Nrg. A cluster of hydrophobic amino acid residues was found near the C-terminus, which might include a transmembrane domain (Fig. 2, amino acid residues in bold italics). MsNrg has an 86 and 57% sequence identity with *M. sexta* Nrg and *D. melanogaster* Nrg, respectively. Protein domain analysis of MsNrg using the NCBI Conserved Domain Search program server revealed that the MsNrg contains six immunoglobulin-like domains, five of which represent IGcam (immunoglobulin cell adhesion molecule domain), and five fibronectin type three (FNIII) domains, from the N- to C-terminus, which are typical of neuroglian family members (data not shown).

Distribution of *MsNrg* mRNA among hemocyte populations and immune stimuli induced changes in the amount of *MsNrg* mRNA

To investigate distribution of *MsNrg* mRNA, we determined mRNA amount in several hemocyte populations using qRT-PCR. First, hemocytes were separated into adhering (granular cells and plasmatocytes) and non-adhering cell types (spherule cells, oenocytoids and prohemocytes), and the total RNA was extracted separately. After reverse transcription, samples were subjected to qRT-PCR, and the initial level of *MsNrg* mRNA was calculated using the 2nd derivative maximum method. Since the mRNA levels of housekeeping genes, namely *RPL32* and *cytoplasmic actin*, differed greatly within each hemocyte category, we used cell numbers to normalize the values for *MsNrg* mRNA. The results are shown in Fig. 3A. The *MsNrg* expression in the adhering hemocytes was as expected but significant levels of expression were unexpectedly recorded in non-adhering hemocytes. Although the MsNrg should have a role in these non-adhering hemocytes, we did not examine this further in this study.

Distribution of *MsNrg* mRNA among adhering hemocytes was analyzed after separation of the different cell types. Hemocyte fractions enriched in granular cells and plasmatocytes were prepared according to our previous paper (Suzuki et al., 2009). Since the procedures for isolating these hemocytes include incubation in the presence either of a growth-blocking peptide or 120 mM EDTA, we do not exclude the possibility that these treatments may alter the expression levels of *MsNrg*. Using respective hemocyte preparations, the levels of *MsNrg* mRNA in the two hemocyte populations were measured (Fig. 3B). Clearly, the *MsNrg* mRNA is much more abundant in plasmatocytes than in granular cells. Furthermore, to confirm whether *MsNrg* was indeed expressed in adhering hemocytes, in situ hybridization was done. Adhering hemocytes were clearly stained when the *MsNrg* anti-sense probe (Fig. 3C) was used, but not stained when the sense probe was used (Fig. 3C). However, clear differences in the intensity of the staining of plasmatocytes and granular cells was not observed.

To confirm whether *MsNrg* mRNA was induced by immune stimuli, intact VI-0 larvae were injected with either formaldehyde-fixed *E. coli* or fluorescent latex beads. Then, we checked the level of *MsNrg* mRNA in both adhering hemocytes and non-adhering hemocytes using qRT-PCR (adhering hemocytes in Fig. 3E and non-adhering hemocytes in Fig. 3F). The results show that the amount of *MsNrg* in adhering hemocytes and non-adhering hemocytes was not changed by the immune stimuli.

Involvement of MsNrg in phagocytosis

The functions of MsNrg protein were analyzed in the context of its involvement in cellular immune defense mechanisms using RNAi. The larvae were injected with dsRNA of either *EGFP* or *MsNrg* and two days later phenotype assays were conducted. For the phagocytosis assay, FITC-labelled *E. coli* was injected into the larval hemo-

Table 1. Proportion of engulfed haemocytes in control and *MsNrg* knockdown larvae.

Injected dsRNA	*EGFP* dsRNA	*MsNrg* dsRNA
Ratio of engulfed hemocytes	0.267 ± 0.0174	0.210 ± 0.0571

p > 0.1 (Mann-Whitney *U* test) based on three replicates. Proportion of haemocytes engulfed = (total number of haemocytes) / (number of engulfed haemocytes). Numbers on the right side of "±" are the S.D.

coel. The larvae were bled 3 h later, the hemocytes were observed with a fluorescent microscope and the percentage of hemocytes that had engulfed the labelled *E. coli* was calculated. Statistical analyses indicated that RNAi of *MsNrg* did not significantly affect the phagocytotic activity more or less than the *EGFP* treatment (Table 1).

Involvement of MsNrg in nodulation

To assess the MsNrg involvement in nodulation, a formaldehyde-fixed *E. coli* suspension was injected into the larvae pre-injected with dsRNA of either *MsNrg* or *EGFP*. The larvae were dissected 24 h later, and numbers and morphology of nodules were examined. No significant difference was found in the number of nodules in the *MsNrg* and *EGFP* dsRNA-treated larvae (Table 2). Nodules dissected under a stereoscopic microscope with Nomarski optics were further observed at a higher magnification. This revealed that the nodules of the *EGFP* dsRNA-treated larvae were morphologically indistinguishable from those from the *MsNrg* dsRNA-treated larvae (data not shown).

Involvement of MsNrg in encapsulation

To evaluate the involvement of the MsNrg in encapsulation, fluorescent latex beads were injected into the VI-0 larvae pre-injected with dsRNA of either *MsNrg* or *EGFP* as above. The larvae were bled 12 h later, and the beads were collected and observed using Nomarski optics. Each bead was classified as representing one of three categories according to the degrees of encapsulation (Fig. 4A–C): (A) fully encapsulated by more than ten cell layers composed of thin, flattened cells; (B) encapsulated by only a few cell layers; (C) only slightly or not encapsulated. Based on the scoring system, the beads recovered from *EGFP* and *MsNrg* dsRNA-treated larvae were classified and counted, and the percentages were calculated. As is evident in Fig. 4D, there was a significant difference in the degree of encapsulation recorded for hemocytes from control *EGFP* and the *MsNrg* dsRNA-treated larvae. In the *EGFP* dsRNA-treated larvae, more than a half of the beads were in category A while in the *MsNrg* dsRNA-treated larvae the peak shifted to category B, indicating that the *MsNrg* RNAi attenuated the encapsulation response. Results presented in Fig. 4D indicate that the injection of *MsNrg* dsRNA consistently reduced the amounts of corresponding mRNA species in adhering hemocytes. To assess the degree of knockdown, the qRT-PCR approach was adopted, and the qRT-PCR revealed that the *MsNrg* knockdown in non-adhering hemocytes did not occur (data not shown). The *MsNrg* mRNA levels in the adhering hemocytes were determined for both *EGFP* and *MsNrg* dsRNA-treated larvae (Fig. 4E). With

Table 2. Number of nodules in control and *MsNrg* knockdown larvae.

Injected dsRNA	*EGFP* dsRNA	*MsNrg* dsRNA
Average number of nodules in larvae	28.3 ± 2.52	33.7 ± 7.64

p > 0.05 (two sample *t*-test), based on three replicates. Numbers on the right side of "±" are S.D.

the knockdown levels around 80% relative to the *EGFP* controls, encapsulation was clearly attenuated in larvae treated with *MsNrg* dsRNA compared to those treated with *EGFP* dsRNA (Fig. 4D).

DISCUSSON

In the present study, the full sequence for *neuroglian* mRNA was obtained from cDNA derived from *M. separata* total hemocytes by combining several reverse transcription and PCR-based methods, including reverse transcription at high temperature. The poly(A) additional signal was AGTAAA, which is atypical. The poly(A) additional signal, however, has many variations and ATGAAA is the one of the variations (Beaudoing et al., 2000). Based on the predicted open reading frame, a full amino acid sequence was obtained and analyzed. MsNrg has six immunoglobulin-like domains and five FNIII domains, which is typical of neuroglian proteins. Neuroglian proteins from *M. sexta* and *D. melanogaster* are reported to bear the same domain structures as MsNrg (Bieber et al., 1989; Chen et al., 1997). The immunoglobulin-like domains have an important role in cell-cell adhesion. In Sf9 cells expressing the *M. sexta Nrg* transgene, cell aggregation was diminished after the addition of monoclonal antibodies that recognize immunoglobulin-like domains of *M. sexta* Nrg (Zhuang et al., 2007). These sequence analysis results imply that the *M. sexta Nrg* functions could be conserved in MsNrg.

MsNrg mRNA was detected in the adhering plasmatocytes and granular cells using qRT-PCR and in situ hybridization. qRT-PCR data show that *MsNrg* mRNA was more abundant in plasmatocytes. Of note is that the *MsNrg* mRNA was also abundant in the non-adhering hemocytes, consisting of spherule cells, oenocytoids and prohemocytes. This was an unexpected result, because the mRNA for this adhesion protein was also expressed in the population of non-adhering hemocytes. At present, we cannot exclude the possibility that the expression level of *MsMrg* might be affected by incubation of hemocytes in culture bottles used for separating adhering and non-adhering hemocytes from total hemocytes. The result implies that *MsNrg* could have unidentified functions in non-adhering hemocytes. Investigation of the functions of *MsNrg* could be a subject for future studies.

Functional assays of MsNrg in terms of its involvement in cellular immune defense were done using the RNAi procedure. As for the involvement in phagocytotic activity, no significant difference was found between the hemocytes from the *MsNrg* dsRNA- and control *EGFP* dsRNA-treated larvae, suggesting that MsNrg may not be involved in phagocytosis. A few immunoglobulin superfamily members have been shown to play a role in phagocytosis in
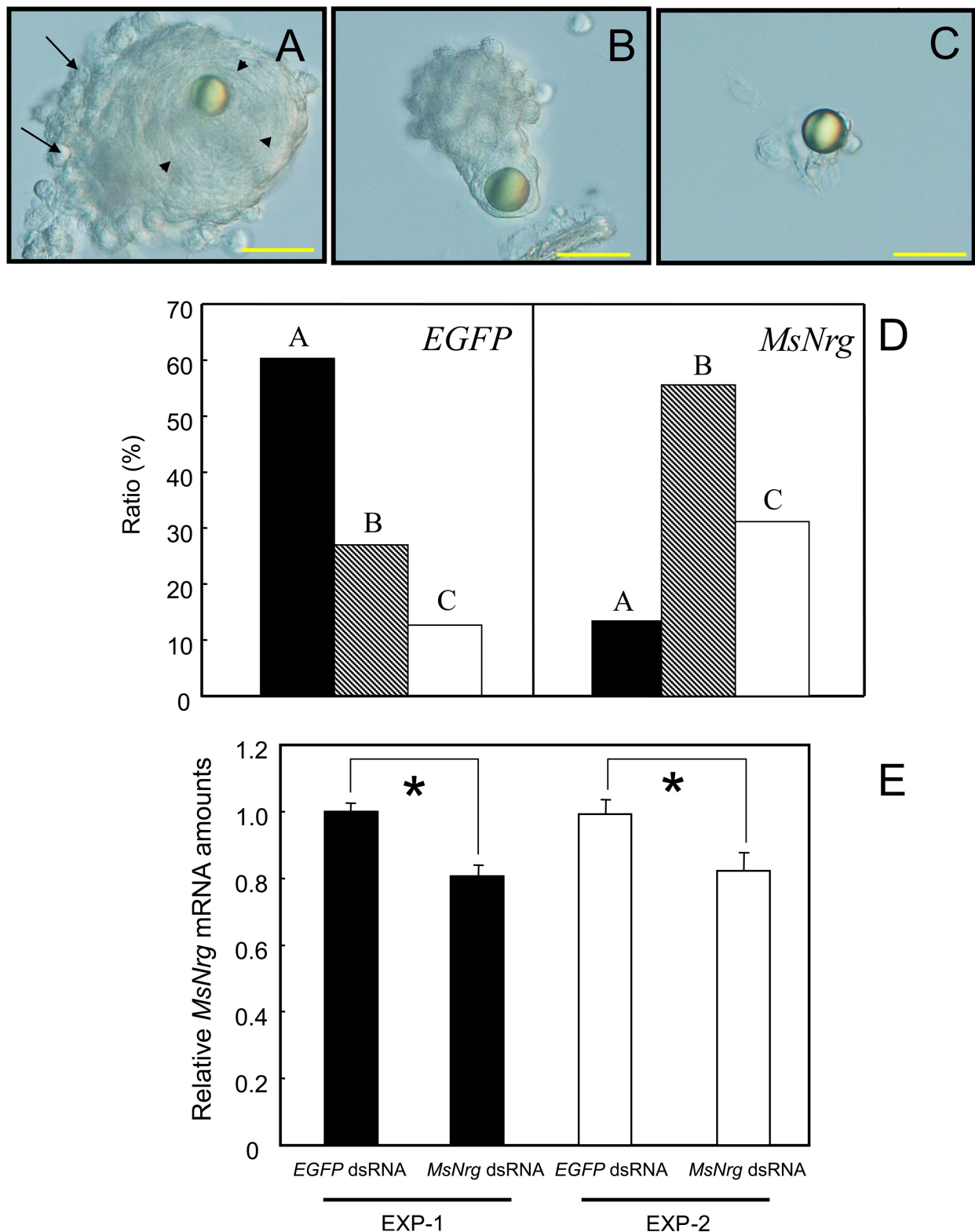
Fig. 4. Scoring the incidence of the encapsulation categories (A–C). Examples of three classes of encapsulated beads are presented. (A) The bead is fully encapsulated with more than 10 layers of thin, flattened cells (arrowheads). Cells with globular shapes form the outer layer (arrows). (B) The bead is surrounded by only a few cell layers. (C) There are either no cells or only a few cells attached to the beads. Scale bars indicate 50 μm. (D) Distribution of encapsulation categories (Fig. 4A–C) for beads recovered from dsRNA-treated larvae. The fluorescent latex beads were collected from the hemocoel of larvae pre-treated with dsRNA of either *EGFP* or *MsNrg*, and the degrees of encapsulation for each bead was determined according to the scoring shown in Fig. 4A–C. The percentages of the respective categories are shown. Three larvae were used for the *EGFP* and *MsNrg* RNAi, and the experiment was repeated three times. Data shown are the sum of the three independent experiments ($p < 0.01$, chi-square test). (E) Changes in levels of *MsNrg* mRNA in adhering hemocytes after dsRNA treatment. Larvae were treated with either *EGFP* or *MsNrg* dsRNA. Two days later, the levels of *MsNrg* mRNA in the adhering hemocytes were determined. The values were normalized based on the number of cells. The experiments were repeated twice, and two sets of results are presented. Sample numbers for each category are three. Asterisks indicate $p < 0.05$ between control and the samples injected with *MsNrg* dsRNA (two sample *t*-test). The average value for *EGFP* in experiment-1 is set to 1.0. Vertical bars represent S.D.

other insects. The Down syndrome cell adhesion molecule (Dscam), which belongs to the immunoglobulin superfamily, functions as a phagocytotic receptor on the surface of *D. melanogaster* hemocytes (Watson et al., 2005). Like neuroglian proteins, Dscam has multiple immunoglobulin-like and FN III domains. Hemolin is another member of immunoglobulin superfamily (Sun et al., 1990), and it occurs only in Lepidoptera. Eleftherianos et al. (2007) report that *Manduca* hemocytes in which hemolin was knocked down took up fewer *E. coli* than the control hemocytes. These other members of the immunoglobulin superfamily (Dscam, hemolin) may also be responsible for phagocytosis by *M. separata* hemocytes.

Significant difference was not found in nodulation between *MsNrg* and *EGFP* dsRNA-treated larvae. The results indicate that MsNrg does not play an indispensable role in nodulation. Data in the literature suggest that cell-cell adhesion is assumed to be an important process in nodulation in which adhering hemocytes play a central role. Nodule formation includes a process of spreading and flattening of plasmatocytes (Dean et al., 2004). Faraldo et al. (2008) present a morphological study showing that nodules consist of spread and non-spread plasmatocytes and granular cells, which are surrounding injected yeast cells. Nodulation is a complex process involving several distinct molecules, such as eicosanoids, prophenoloxidase and dopadecarboxylase, in addition to adhesion molecules (Marmaras & Lampropoulou, 2009). During the process of cell-cell adhesion in nodulation, several distinct adhesion molecules may participate. Under such circumstances, the RNAi knockdown effect on one adhesion molecule could be rescued by the redundancy provided by other molecular species. Therefore, we cannot exclude the functional involvement of MsNrg in nodulation, even though attenuation of nodulation was not observed after treatment with *MsNrg* RNAi. The degree of *MsNrg* knockdown was moderate after the dsRNA treatment. This moderate knockdown brought about a clear shift in phenotype for encapsulation, but not for nodulation. This may reflect the involvement of multiple adhesion molecules in the process of cell-cell adhesion during nodulation. The possibility that more effective *MsNrg* knockdown might result in clearer changes in nodulation phenotypes also exists.

The encapsulation of injected latex beads by hemocytes was weakened by the *MsNrg* dsRNA treatment. The degree of attenuation is modest, which may correspond to the modest, 80% relative to the control, *MsNrg* knockdown determined by qRT-PCR. Microscopic observation revealed that after *MsNrg* dsRNA treatment the numbers of beads surrounded by multiple layers of thin, flattened cells decreased significantly and consistently. According to morphological features of these cells, the thin and flattened cells were probably plasmatocytes (Lavine & Strand, 2002). In *M. sexta,* when the larvae were treated with *M. sexta Nrg* dsRNA, the numbers of fully encapsulated Sephadex beads decreased to 50% (Zhuang et al., 2007). In *D. melanogaster*, improper encapsulated wasp eggs were observed in *D. melanogaster* expressing mutant *Nrg* (Wil-

liams, 2009). Our result and the two reports for *M. sexta* and *D. melanogaster* suggested that the cellular immunological role of neuroglian was conserved within Lepidoptera and *D. melanogaster*.

We show that MsNrg is involved in encapsulation of latex beads (abiotic targets), which indicates that MsNrg is involved in the cellular immune reaction against abiotic targets. Williams (2009) shows that a mutant of *Nrg* in *Drosophila* incompletely encapsulated parasitoid wasp eggs (biotic targets). Considering both this report and our results, MsNrg can function against both biotic and abiotic targets in at least encapsulations.

The qRT-PCR revealed an abundance of *MsNrg* mRNA in plasmatocytes, three-times more abundant than in granular cells. When the larvae were treated with *MsNrg* dsRNA, the percentage of fully encapsulated fluorescent latex beads decreased to less than 25% of the control. Assays using qRT-PCR showed that the associated level of knockdown was only modest (Fig. 4E). This indicates that an efficient knockdown might occur in some *MsNrg*-expressing subpopulations of plasmatocytes, which are involved in encapsulation. Given these results, MsNrg is likely to function as major adhesion molecule in the formation of multiple plasmatocyte layers surrounding large invading non-selves. We did these mRNA quantifications without separating adhering hemocytes into populations of granular cells and plasmatocytes, since the separation procedures require long incubation periods and relatively severe treatments (Suzuki et al., 2009), which could affect gene expression.

In this study we determined the distribution and levels of expression of *MsNrg* mRNA mainly in hemocyte preparations consisting of two or more types of cells using qRT-PCR and in situ hybridization. These results revealed the *MsNrg* was expressed not only in adhering hemocytes but also in non-adhering hemocytes, which are not thought to be involved the cellular immune reactions. In addition, we revealed using RNAi that MsNrg was involved in the cellular immune reaction, encapsulation. Our results showed that neuroglian could have unidentified function in non-adhering hemocytes, and the cellular immunological function of neuroglian is conserved within Lepidoptera and *D. melanogaster*.

REFERENCES

BEAUDOING E., FREIER S., WYATT J.R., CLAVERIE J.M. & GAUTHERET D. 2010: Patterns of variant polyadenylation signal usage in human genes. — *Genome Res*. **10**: 1001–1010.

BIEBER A.J., SNOW P.M., HORTSCH M., PATEL N.H., JACOBS J.R., TRAQUINA Z.R., SCHILLING J. & GOODMAN C.S. 1989: *Drosophila* neuroglian: a member of the immunoglobulin superfamily with extensive homology to the vertebrate neural adhesion molecule L1. — *Cell* **59**: 447–460.

CHEN C.L., LAMPE D.J., ROBERTSON H.M. & NARDI J.B. 1997: Neuroglian is expressed on cells destined to form the prothoracic glands of *Manduca* embryos as they segregate from surrounding cells and rearrange during morphogenesis. — *Dev. Biol.* **181**: 1–13.

DA SILVA J.B., DE ALBUQUERQUE C.M., DE ARAUJO E.C., PEIXOTO C.A. & HURD H. 2000: Immune defense mechanisms of *Culex quinquefasciatus* (Diptera: Culicidae) against *Candida albicans* infection. — *J. Invertebr. Pathol.* **76**: 257–262.

DEAN P., RICHARDS E.H., EDWARDS J.P., REYNOLDS S.E. & CHARNLEY K. 2004: Microbial infection causes the appearance of haemocytes with extreme spreading ability in monolayers of the tobacco hornworm *Manduca sexta*. — *Dev. Comp. Immunol.* **28**: 689–700.

ELEFTHERIANOS I., GÖKÇEN F., FELFÖLDI G., MILLICHAP P.J., TRENCZEK T.E. FRENCH-CONSTANT R.H. & REYNOLDS S.E. 2007: The immunoglobulin family protein Hemolin mediates cellular immune responses to bacteria in the insect *Manduca sexta*. — *Cell Microbiol.* **5**: 1137–1147.

FARALDO A.C., GREGORIO E.A. & LELLO E. 2008: Morphological and quantitative aspects of nodule formation in hemolymph of the blowfly *Chrysomya megacephala* (Fabricius, 1794). — *Exp. Parasitol.* **118**: 372–377.

HALL S.G. & BIEBER A.J. 1997: Mutations in the *Drosophila* neuroglian cell adhesion molecule affect motor neuron pathfinding and peripheral nervous system patterning. — *J. Neurobiol.* **32**: 325–340.

HERNANDEZ S., LANZ H., RODRIGUEZ M.H., TORRES J.A., MARTINEZ-PALOMO A. & TSUTSUMI V. 1999: Morphological and cytochemical characterization of female *Anopheles albimanus* (Diptera: Culicidae) hemocytes. — *J. Med. Entomol.* **36**: 426–434.

HORTSCH M. 1996: The L1 family of neural cell adhesion molecules: Old proteins performing new tricks. — *Neuron* **17**: 587–593.

HORTSCH M., WANG Y.M., MARIKAR Y. & BIEBER A.J. 1995: The cytoplasmic domain of the *Drosophila* cell adhesion molecule neuroglian is not essential for its homophilic adhesive properties in S2 cells. — *J. Biol. Chem.* **270**: 18809–18817.

KATO Y., YOSHIDA T., MIURA K., TANAKA T., NAKAMATSU Y. & OCHIAI M. 2014: A novel type of hemocytes localizing melanization with high-spreading behavior in *Mythimna separata*. — *Arch. Insect Biochem. Physiol.* **86**: 220–239.

LAVINE M.D. & STRAND M.R. 2002: Insect hemocytes and their role in immunity. — *Insect Biochem. Mol. Biol.* **32**: 1295–1309.

LEMAITRE B. & HOFFMANN J. 2007: The host defense of *Drosophila melanogaster*. — *Annu. Rev. Immunol.* **47**: 697–743.

MARCHLER-BAUER A., BO Y., HAN L., HE J., LANCZYCKI C.J., LU S., CHITSAZ F., DERBYSHIRE M.K., GEER R.C., GONZALES N.R. ET AL. 2017: CDD/SPARCLE: Functional classification of proteins via subfamily domain architectures. — *Nucl. Acids Res.* **45**: D200–D203.

MARMARAS V.J. & LAMPROPOULOU M. 2009: Regulators and signalling in insect hemocyte immunity. — *Cell Signal.* **21**: 186–195.

NAKAMATSU Y., KURIYA K., HARVEY J.A. & TANAKA T. 2006: Influence of nutrient deficiency caused by host developmental arrest on the growth and development of a koinobiont parasitoid. — *J. Insect Physiol.* **52**: 1105–1112.

NARDI J.B. 1994: Rearrangement of epithelial cell types in an insect wing monolayer is accompanied by differential expression of a cell surface protein. — *Dev. Dyn.* **199**: 315–325.

NARDI J.B., PILAS B., UJHELYI E., GARSHA K. & KANOST M.R. 2003: Hematopoietic organs of *Manduca sexta* and hemocyte lineages. — *Dev. Genes Evol.* **213**: 477–491.

NARDI J.B., ZHUANG S., PILAS B., BEE C.M. & KANOST M.R. 2005: Clustering of adhesion receptors following exposure of insect blood cells to foreign surfaces. — *J. Insect Physiol* **51**: 555–564.

NARDI J.B., PILAS B., BEE C.M., ZHUANG S., GARSHA K. & KANOST M.R. 2006: Neuroglian-positive plasmatocytes of *Manduca sexta* and the initiation of hemocyte attachment to foreign surfaces. — *Dev. Comp. Immunol.* **30**: 447–462.

SIEGENTHALER D., ENNEKING E.M., MORENO E. & PIELAGE J. 2015: L1CAM/Neuroglian controls the axon-axon interactions establishing layered and lobular mushroom body architecture. — *J. Cell Biol.* **208**: 1003–1018.

SUN S.C., LINDSTROM I., BOMAN H.G., FAYE I. & SCHMIDT O. 1990: Hemolin: An insect-immune protein belonging to the immunoglobulin superfamily. — *Science* **250**: 1729–1732.

SUZUKI M. & TANAKA T. 2007: Development of *Meteorus pulchricornis* and regulation of its noctuid host, *Pseudaletia separata*. — *J. Insect Physiol.* **53**: 1072–1078.

SUZUKI M., MIURA K. & TANAKA T. 2008: The virus-like particles of a braconid endoparasitoid wasp, *Meteorus pulchricornis*, inhibit hemocyte spreading in its noctuid host, *Pseudaletia separata*. — *J. Insect Physiol.* **54**: 1015–1022.

SUZUKI M., MIURA K. & TANAKA T. 2009: Effects of the virus-like particles of a braconid endoparasitoid, *Meteorus pulchricornis*, on hemocytes and hematopoietic organs of its noctuid host, *Pseudaletia separata*. — *Appl. Entomol. Zool.* **44**: 115–125.

WATSON F.L., PUTTMANN-HOLGADO R., THOMAS F., LAMAR D.L., HUGHES M., KONDO M., REBEL V.I. & SCHMUCKER D. 2005: Extensive diversity of Ig-superfamily proteins in the immune system of insects. — *Science* **309**: 1874–1878.

WIEGAND C., LEVIN D., GILLESPIE J., WILLOTT E., KANOST M.R. & TRENCZEK T. 2000: Monoclonal antibody MS13 identifies a plasmatocyte membrane protein and inhibits encapsulation and spreading reactions of *Manduca sexta* hemocytes. — *Arch. Insect Biochem. Physiol.* **45**: 95–108.

WILLIAMS M.J. 2009: The *Drosophila* cell adhesion molecule Neuroglian regulates Lissencephaly-1 localisation in circulating immunosurveillance cells. — *BMC Immunol.* **10**: 17, 12 pp.

ZHUANG S., KELO L., NARDI J.B. & KANOST M.R. 2007: Neuroglian on hemocyte surfaces is involved in homophilic and heterophilic interactions of the innate immune system of *Manduca sexta*. — *Dev. Comp. Immunol* **31**: 1159–1167.